UCRL-JRNL-228467

LAWRENCE
LIVERMORE
NATIONAL
LABORATORY

Ramp Compression Experiments - a Sensitivity Study

M. Bastea, D. Reisman

February 28, 2007

Proceedings of the International Conference on Shock Compression of Condensed Matter

Disclaimer

This document was prepared as an account of work sponsored by an agency of the United States government. Neither the United States government nor Lawrence Livermore National Security, LLC, nor any of their employees makes any warranty, expressed or implied, or assumes any legal liability or responsibility for the accuracy, completeness, or usefulness of any information, apparatus, product, or process disclosed, or represents that its use would not infringe privately owned rights. Reference herein to any specific commercial product, process, or service by trade name, trademark, manufacturer, or otherwise does not necessarily constitute or imply its endorsement, recommendation, or favoring by the United States government or Lawrence Livermore National Security, LLC. The views and opinions of authors expressed herein do not necessarily state or reflect those of the United States government or Lawrence Livermore National Security, LLC, and shall not be used for advertising or product endorsement purposes.

Ramp Compression Experiments - a Sensitivity Study

Marina Bastea[1] and David Reisman
[1] *Lawrence Livermore National Laboratory, Livermore, CA 94550, USA*
(Dated: February 26, 2007)

We present the first sensitivity study of the material isentropes extracted from ramp compression experiments. We perform hydrodynamic simulations of representative experimental geometries associated with ramp compression experiments and discuss the major factors determining the accuracy of the equation of state information extracted from such data.

PACS numbers: 64.30.+t, 62.50.+p, 07.35.+k

A wealth of experimental high pressure studies have been aimed in the last decades at understanding the fundamental behavior of matter under compression. Many of them employed well established techniques operating under either static - diamond anvil cell (DAC)[1] or dynamic - shock Hugoniot [2] high-pressure conditions. More recent technical advancements however have also made possible the study of new dynamic regimes by spreading the pressure loading from near-instantaneous, i.e. shock, to tens, hundreds and even thousands of nanoseconds, through the use of laser [3], electromagnetic [4] and graded density impactor (GDI) [5, 6] techniques respectively. The emergence of ramp compression methods affords new opportunities for advancing the very active field of high pressure physics but also poses challenges related to the development and validation of suitable design and analysis methodologies. Already new results regarding the high pressure equation of state (EOS) of materials [7–10] as well as the kinetics of phase transformations [11–13] stem from the use of these techniques.

Ramp compression experiments have the potential to reveal the behavior of matter compressed along a quasi-isentrope thereby adding a new dimension to the experimentally accessible high pressure thermodynamic regimes. It is therefore critical that the accuracy of the stress/density results derived from such measurements be thoroughly assessed. The present work is the first study of the sensitivity of the equation of state (EOS) information extracted from ramp compression experiments on the major sources of experimental uncertainties. These sources are grouped into three categories: sample package metrology (e.g. anode, glue bond and sample thicknesses), *in-situ* diagnostics (e.g. VISAR timing and velocity) and pressure ramp uncertainties. We evaluated their contributions separately using 1D standard hydrodynamic simulations of a typical experimental geometry used in **mag**netically-driven **i**sentropic **c**ompression (MAGIC) experiments [8–10] and Lagrangian analysis to extract the stress-density information from the simulation results. Magnetic pulsers such as the Z accelerator, operate on intermediate time and length scales bridging the typical laser and gas-gun (GDI) regimes. The results may naturally be extrapolated in either direction to draw conclusions specific to both laser or GDI generated ramps, as appropriate.

In a typical EOS experiment, regardless of the $P(t)$ ramp generation method used, the experimental observables are the velocity histories at the free (or windowed) surfaces of usually 2-4 samples of different thicknesses. Ideally these samples are dynamically compressed according to identical, prescribed loading paths [7–10, 14]. We mimicked the experiments with simulations of a basic geometry consisting of a 0.7 mm copper layer (representing the anode) followed by a tantalum (Ta) sample. We applied a pressure ramp $P(t)$, to the left boundary of the Cu and computed the free surface velocity of the Ta sample - $u(t)$, see Fig. 1. Each test case discussed below consisted of four simulations, denoted by Si, $i = \overline{1,4}$, corresponding to Ta samples of thicknesses th$_i$ = 400, 500, 600 and 700 μm respectively, one or several of which were slightly altered to reflect each of the studied uncertainties. The copper was described by QEOS [15] while the samples were modeled using Mie-Gruneisen analytic forms based on the data summarized in Ref. [16]. Stress-density information was extracted from the computed velocity histories using Lagrangian analysis, as described below, and compared with the sample EOS input of the simulations.

Since in ramp loading experiments sample compression is achieved gradually over tens to thousands of nanoseconds as illustrated in the inset to Fig. 1 [14] (note the smooth, gradual rise in the experimental traces), it is assumed that the thermodynamic path followed by the material is nearly isentropic. This allows the determination of the material specific stress-strain relationship by using the free-surface velocities $u_i(t)$ corresponding to different sample thicknesses. The algorithm used to extract the material isentrope assumes that the stress history at a certain depth inside the target and at early enough times is identical for all samples and that the state information is carried to the measurement surface at the sound speed. In the present study loading histories are assumed identical at the Cu/Ta interface. No non-equilibrium or rate effects are taken into consideration. Generally, in ramp compression experiments the wave interactions are extremely complex, e.g. waves reflected at the measurement surface interact with later portions of the arriving ramp compression and produce distortions of

the stress experienced by samples of different thicknesses. Proper consideration of these interactions constrains for example the setting of the optimization intervals in the inversion algorithms (see below). Two methods are currently available for extracting the material stress-strain relationship along the uniaxial compression path: Iterative Lagrangian analysis (*ILA*) described in [17], and Reverse Integration and Optimization (*RIO*), which we used in the present study, as outlined below. The *RIO* and *ILA* yield results in excellent agreement; for a discussion see for example Ref. [14].

The *RIO* method assumes a certain parametrization of the material EOS and integrates the mass and momentum conservation equations in the negative direction along the Lagrangian spatial coordinate from the free surface (or window) to the reference surface. This yields an applied longitudinal stress history $\sigma_{li}(t)$ for each sample i. The root-mean-square deviation of these stress histories from combinations of different samples normalized by their average $(\sigma_{li} - \sigma_{lj})/(\sigma_{li} + \sigma_{lj})$ is then minimized while varying material EOS parameters, consistent with the assumption of identical applied pressures $P(t)$. For the present inversions the Ta equation of state was represented by a ratio of polynomials:

$$\rho = \rho_o \frac{1 + \sum_{j=1}^{3} b_j \sigma^j}{1 + \sum_{j=1}^{2} a_j \sigma^j}; \qquad (1)$$

where $\sigma = \sigma_l - P_o$ and ρ_o, P_o are the ambient density and pressure. The onset of divergences in the pressure loading histories is a good indicator for the occurrence of wave interactions - and this is what we used in our analysis to set the appropriate time domain for the minimization. Minimizations were performed on combinations of two, three and all four samples (simulations). We confirmed both that the inverted isentropes reproduce the ideal simulation input and that the result is robust, e.g. starting from completely different EOS curves yields negligible differences in the final result. We also tested that different EOS parameterizations with comparable degrees of freedom give virtually identical *RIO* results. The stress/density curves shown in Figs. 2- 5 are indexed by the respective simulations used in the minimization.

We now proceed to explore the effects of various uncertainties related to target metrology/ assembly, experimental diagnostics and pressure generator performance on the material isentrope extracted using the above Lagrangian analysis. In the Z experiments the pressure wave is typically launched first through the Cu metallic anode to which the samples are attached. The anode thickness at each sample location is therefore one of the critical factors in determining the outcome of the experiments. Variations in thickness are quite common ($\sim 1 - 5\mu m$) and are mainly caused by imperfections in the fabrication process. Similar considerations apply to the GDI technique. The relatively large samples used in MAGIC and GDI experiments, while easing the assembly and handling processes, create difficulties for maintaining the flatness and parallelism tolerances across large surfaces. To assess the impact of such a condition, the Cu layer in simulation S1, (with a $400\mu m$ sample) was increased to $705\mu m$ instead of the $700\mu m$ used in S2-4. Identical current/pressure pulses were applied at the left boundary of the Cu for all four cases. The inversion results shown in Fig. 2(a) exhibit a spread of $\sim 12\%$ in the pairwise results and a $\sim 4\%$ deviation of the average isentrope from the simulation input. We note that, as expected, results from pairs that do not include S1 yield the ideal isentrope, i.e. the simulation input. The impact of anode thickness non-uniformity may be minimized if properly diagnosed before the experiment, by applying a time correction to the $u(t)$ history. Although a simple time-shift would be a good first approximation, an accurate correction has a definite non-linear, time dependent component which may be calculated assuming that the EOS for the anode material is well understood and the size deviation has been measured prior to the experiment.

The presence of intermediate layers for bonding/transition purposes inside the targets is also a common occurrence in ramp compression experiments. These layers are typically less than 2 μm, $\leq$ 0.5% of the sample thickness, and are poorly characterized due to significant technical difficulties. Bonding may be required at the sample interfaces with either the base-plate (panel) or any window present in the experiments (GDI or MAGIC). The laser ramping techniques use deposition methods to create the sample on top of a window. In such cases it is reasonable to expect that the transition to standard bulk properties of the sample occurs over $\sim 1000\mathring{A}$, still approximately .3% of a 30μm typical sample size. In order to quantify these effects we introduced a $5\mu m$ glue layer (effectively 5% of the 100 μm step size) in S1 between the Cu anode and the sample. This is an overestimate of the state-of-the-art experiments, and was chosen for illustration purposes only. The resulting u_1(t) was inverted in combination with the ideal (no glue) S2-4 simulations results. Similar to the previous case, a large spread was observed in the pair-wise inverted isentropes, and a 5% deviation of the average result from the input isentrope. We note that the effect of adding an identical glue layer to *all* simulations (i.e. S1-4) is significantly smaller. We may conclude that for improving the accuracy of EOS data it is highly desirable to enlarge the ratio between the step-size and intermediate layer thickness which ultimately controls it's impact. In laser driven ramp compression experiments, for example, typical step-sizes between samples are ten times smaller than in the test case presently discussed, of order $\sim 10\mu m$, and a transitional layer of $0.5\mu m$ would produce inversion errors similar with the ones discussed here. For the GDI

experiments the sample steps are larger but the use of additional bonding to windows has to be taken into account.

The sample thickness, parallelism and surface finish also play a critical role in determining the accuracy of the extracted EOS and are common issues to all the techniques. To test such effects we introduced a 1% error for the $400\mu m$ sample thickness. The results, see Fig. 2(b), exhibit a sizable spread in the pairwise analysis as well as an $\sim 4\%$ overall shift of the final, average inverted isentrope. We note that the effect of thickness uncertainties significantly diminish as the sample steps increase; e.g. the S1/S4 (400 and 700 μm respectively) pair yields results closer to the unperturbed S2/S3/S4 combinations than the S1/S2 pair. This is illustrated in the inset to Fig 2b and shows that the error is essentially controlled by the relationship between the thickness uncertainty and the step size. This result suggests special constraints for laser driven ramp-compression experiments where typical step sizes are of the order of $10\mu m$ requiring therefore precisions of order $\sim 100nm$. The requirements are significantly easier to meet in GDI experiments which usually use larger samples and steps.

We next proceed to discuss the precision of the VISAR diagnostics employed in the experiments as it impacts the accuracy of the results. The velocity of each sample free-surface, $u(t)$, is typically monitored during compression with at least two VISAR channels of different sensitivities. An average of the measured experimental records may therefore be computed for each sample, and used in the inversion analysis. Timing of individual channels at Z is generally determined with an accuracy of $\simeq 0.25ns \sim 0.1\%$ of the ramp rise time; this value is consistent with the temporal spread observed in actual individual experimental traces. The error in velocity attributable to the measurement of the Doppler shift is approximately 2% of the sensitivity settings [21], which may be as low as .2km/s/fr at the Z-accelerator for example. Fig. 3 shows the inversion result following a global $1ns$ shift applied to $u_1(t)$, the velocity trace computed in S1 ($400\mu m$ sample), indicating an EOS error of $\simeq 5\%$. A systematic time shift introduced identically in all $u_i(t)$ traces produced little differences from the ideal case. Generally for laser driven ICE, the timing accuracy is determined by the resolution of streak-cameras to $\simeq 20-50ps \sim 0.5\%-1\%$ of the overall rise time [7], comparable with the performance of point-VISARs employed in the other techniques.

Although none of the Z-accelerator studies to date experimentally diagnosed or explicitly documented any pressure pulse generation uncertainties, e.g. systematic misalignment of the anode-cathode (AK) or local fluctuations of the loading pressure, we tested this possibility as well. To guide this analysis we referred to both laser shock experiments, where 2% fluctuations in pressure have been diagnosed under direct drive conditions [19], and observations of inter-panel pressure variations encountered in other low pressure experiments at Z [20]. We find for example that enhancing by 2% the pressure pulse that compresses the $500\mu m$ sample (simulation S2) alone appears to generate a large spread in the pairwise results, although coincidentally leaving the average all-sample stress/density curve unchanged, see Fig. 4a. Applying the same pressure scaling factor to another simulation (S4) produces a similar scatter in the pairs analysis and also a large deviation of the average inversion.

The alignment between the anode and cathode determines the characteristics of the compression pulse generated by the electromagnetic discharge. Non-parallelism of the anode/cathode (A/K) assembly, even on a local scale, is a complex, multi-dimensional magneto-hydrodynamic problem which will affect the outcome of the entire experiment, albeit at different levels. We conducted a simplified, first order analysis of such an effect by enhancing the applied pressure $P_i(t)$ in S2-4 by 1%, 2% and 3% respectively. Since $P \sim 1/(x)^2$, where x is the AK gap, this essentially corresponds to modifying the AK gaps to 0.995mm in S2, 0.99mm in S3 and 0.985mm in S4 from the nominal 1mm value. The inversion results in this case are consistently stiffer - no spreading is observed in the pairwise or triplet results. An apparent softening of the inversion results may be produced if the pressure is correspondingly lowered, i.e. the AK gap is progressively enlarged. Furthermore, increases of the pressure scaling factor translate nearly-linearly into the deviations of the inverted isentropes, see Fig. 5. Placing two samples of identical thickness at opposite ends of the panel, where effects of such systematic angular deviations are expected to be largest can provide the means to quantify the magnitude of the condition and a basis to develop corrections for it.

In conclusion, we analyzed both qualitatively and quantitatively the major experimental factors that determine the accuracy of equations of state extracted from ramp compression experiments. Since in actual experiments essentially all the effects discussed here will compound, factoring out individual signatures and magnitudes, as done in the present work, is especially important. This study should provide some guidance for the effective design and analysis of ramp compression experiments, as well as for further improvements of ramp generators performance.

We thank N. Holmes, S. Rothman, J. Eggert, R. Smith and J.P. Davis for useful discussions. This work was performed under the auspices of the U.S. Department of Energy by University of California Lawrence Livermore National Laboratory under Contract No. W-7405-Eng-48.

[1] *Elastic properties and equations of state* Edited by

Thomas J. Shankland and Jay D. Bass (AGU 1989) and refs. therein.
[2] A.C. Mitchell and W.J. Nellis, J. Appl. Phys. **52**, 3363(1981); N.C. Holmes, J.A. Moriarty, G.R. Gathers, and W.J. Nellis, J. Appl. Phys. **66**,2962(1989)
[3] J. Edwards et al., Phys. Rev. Lett. **92**, 0750021 (2004).
[4] C.A.Hall et al., Rev. Sci. Instrum. **72** 3587 (2001).
[5] L.C. Chhabildas, J.R. Asay and L.M. Barker, *Shear Strength of Tungsten under Shock and Quasi-isentropic Loading to 250 GPa*, SNL report SAND88-0306-UC34 (1988).
[6] J.H. Nguyen, D. Orlikowski, F.H. Streitz, N.C. Holmes, J.A. Moriarty, AIP Conference Proceedings, **706**, 1225 (2004).
[7] R. Smith et al., Phys. Rev. Lett. **98**, 065701 (2007).
[8] M. Knudson et al., Phys. Rev. Lett. **90** 035505 (2003).
[9] D. Hayes et al., J. Appl. Phys. **96** 5520 (2004).
[10] J-P. Davis, J. Appl. Phys. **99**, 103512(2006).
[11] M. Bastea et al., Phys. Rev. B **71** 180101 (2005).
[12] M. Bastea et al., submitted to Phys. Rev. Lett. (2006).
[13] M. Bastea and D. Reisman, submitted to Appl. Phys. Lett. (Feb 2007).
[14] M. Bastea et al. *High-pressure Ramp Compression of Tantalum*, LLNL report UCRL-JRNL-221843-DRAFT.
[15] R.M. Moore et al, Phys Fluids **31**, 3059 (1988).
[16] S.P. Marsh, *LASL Shock Hugoniot Data* (University of California Press, Berkeley, 1980).
[17] S. Rothman et al., J. Phys.D-Appl. Phys., **38** 733 (2005).
[18] R. Fowles and R.F. Williams, J.Appl.Phys. **41** 360(1970); M. Cowperthwaite and R.F. Williams, J.Appl.Phys. **42** 456(1971); L.Seaman, J.Appl.Phys. **45** 4303(1974); J.B. Aidun and Y.M. Gupta, J.Appl.Phys. **69** 6998(1991).
[19] P. Celliers et al., Phys. of Plasmas **11** (2004).
[20] M. Bastea and D. Reisman, submitted to Appl. Phys. Lett. (2007).
[21] Hemsing, Rev. Sci. Instr. **50** 73(1979); L.M.Barker *Shock Compression of Condensed Matter - 1997* edited by S.C. Schmidt, D.P.Dandekar and J.W.Forbes (American Institute of Physics, Woodbury, NY, 1998), pp.833-6.

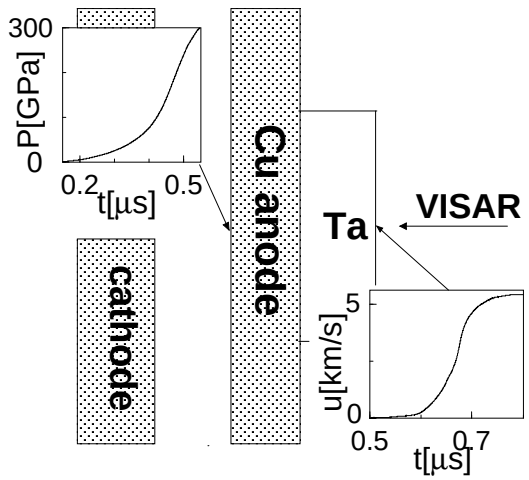

FIG. 1: Schematic cross-section (not to scale) of the simulated geometry emulating a typical Z-accelerator experimental setup: 2mm thick tungsten cathode, 0.7mm copper anode separated from the cathode by a 1mm vacuum gap, and Ta samples of various thicknesses. Velocity of the Ta free surface is measured during compression using VISAR. Also shown as inset is a typical shockless loading curve $P(t)$ generated by the electromagnetic discharge at the left boundary of the anode and a sample velocity curve u(t) measured in one of our experiments.

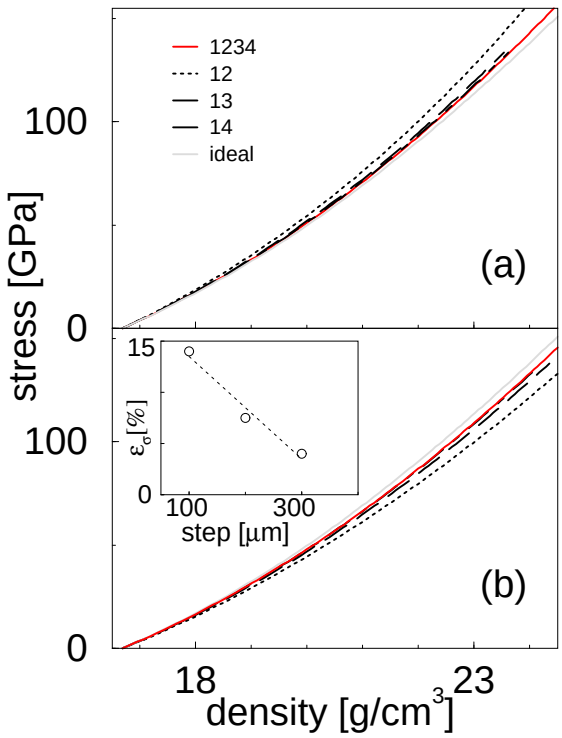

FIG. 2: Sensitivity of the inverted isentrope to anode (a), and sample (b) thicknesses as described in text. Curves are indexed by the simulations used in the inversion process. Inset: error in the pairwise inverted isentrope ($\sigma_{ij}/\sigma_{id} - 1$) as a function of step size (th$_j$-th$_i$).

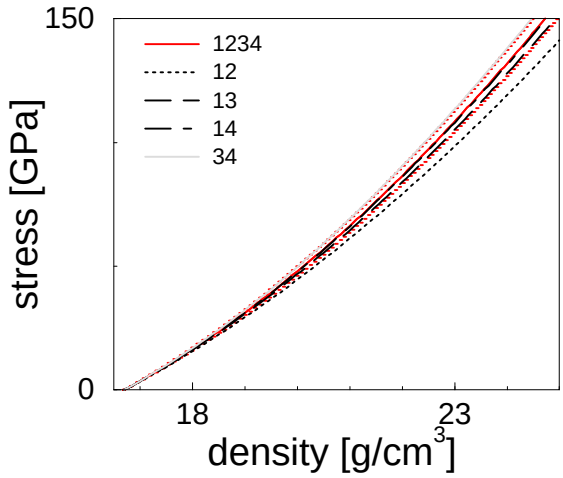

FIG. 3: Sensitivity to timing accuracy - a 1 ns time error was introduced in simulation S1, (400μm sample). A 4% error margin, dotted red, is shown around the average inverted isentrope.

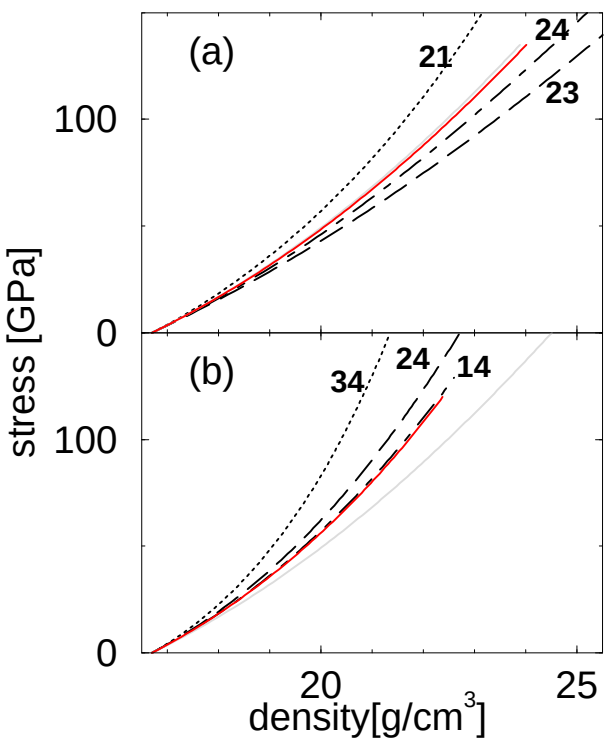

FIG. 4: Effects of local pressure scaling - in each set of simulations one pressure drive was enhanced by 2% while the other three were maintained unchanged. Results of pressure scaling applied to simulations S2 and S4 are shown in (a) and (b) respectively. The gray line is the ideal extracted isentrope - from samples with identical drive which coincides with the material isentrope used in the hydrodynamic simulations. The red line is the inversion result using all four simulations.

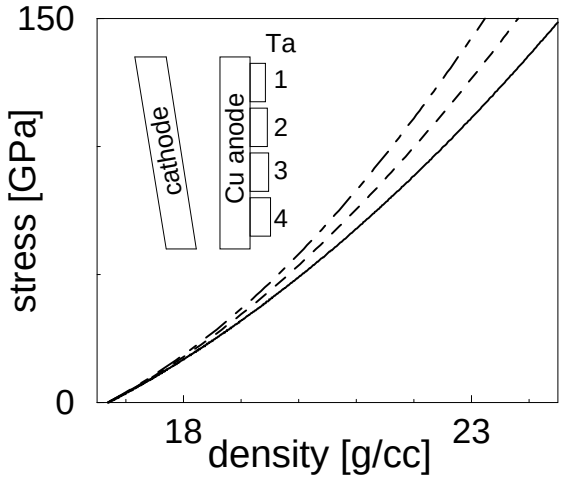

FIG. 5: Continuous line - ideal isentrope used in hydro-simulations. Dotted and dashed lines - inversion results using simulations with 1% and 2% cumulative pressure increments at each sample location, respectively.